



A MODIFIED ENTRAINMENT COEFFICIENT RELATION FOR THE DESCRIPTION OF THE COANDA EFFECT ON BUBBLE PLUMES

Philippe P. M. Menut, Jian Su†,

and Atila P. Silva Freire

Mechanical Engineering Program (PEM/COPPE/UFRJ),

C.P. 68503, 21945-970 - Rio de Janeiro - Brazil.

†Nuclear Engineering Program (PEN/COPPE/UFRJ),

C.P. 68509, 21945-970 - Rio de Janeiro - Brazil.

Abstract. *This paper describes the gas fraction distribution in the two-phase flow of a gas-liquid bubble plume set to develop adjacent to another bubble plume. When this happens, the plume exhibits a type of Coanda effect, bending towards the other plume. The local gas fraction measurements are carried out using the electro-resistivity probe technique in an air-water system. The deflection angle of the plumes is shown to present a logarithmic dependence on the modified Weber and Froude numbers of the flow. In addition, a simple theory based on integral methods is advanced for the prediction of the plume deflection; the theory considers a variable entrainment coefficient.*

Key words: *Bubble plume, Coanda effect, entrainment coefficient.*

INTRODUCTION

In a host of industrial processes, gas bubbling in confined spaces is used to promote the chemical and thermal homogenization of mixtures. The central question in gas stirring operations is to identify procedures and equipment that provide the maximum possible homogenization in the minimum time.

The purpose of this work is to investigate the behaviour that plumes set side by side will have as a function of the gas source characteristics. When two plumes are arranged in this geometry, they tend to bent towards each other. The tendency of a fluid, either gaseous or liquid, to cling to a vertical surface that is near to an orifice from which the fluid emerges is called the Coanda effect. This denomination has also been widely used to describe the attraction effects that flows issuing from adjacent orifices exert on each other. Here, we will show that the bending is provoked by an inhibition in part of the entrainment of external fluid by the mean flow.

In many situations, bubble plumes can be described through the two-dimensional

continuity and momentum equations, expressed in cylindrical polar coordinates. While many flows can be thought as having an axisymmetric form, a major feature of industrial flows is their three dimensional character. This feature is further enhanced when the source of gas is located close to a wall or close to another source, so that the Coanda effect sets in. The present work will make use of a simple integral formulation to capture all relevant features of the flow. The theory is an extension of the procedure of Ditmars and Cederwall(1974), making use, for the sake of simplicity, of Gaussian profiles and of Boussinesq assumption. The theory makes simple considerations about the conservation of the entrained momentum and proposes a new expression for the description of the entrainment coefficient as a function of the Weber number.

The flow properties will, of course, depend on the specific manner in which gas is injected in the considered vessel. For most studies, just a single source of gas is considered, which gives rise to a flow that can be considered axisymmetric. This is, in fact, a mandatory procedure when an integral approach to the problem is used and the entrainment hypothesis considered. Here we will consider that the deflection of the plume is small enough so that Gaussian profiles can still be applied to the problem.

The numerical results are compared with a set of experiments carried out for a twin-plume arrangement. The local gas fraction measurements are carried out using the electro-resistivity probe technique in an air-water system. The system comprises a 1 m^3 volume water tank and air injection nozzles whose flow rates range from 1.8 to 10.7 litre per minute. Results are presented for the void fraction, and velocity profiles. By an analysis of the experimental data through the void fraction profiles, the deflection of the plume has been evaluated as a function of several parameters of interest including the gas flow rate and the distance between the point sources.

The single bubble plume flow has been extensively studied both theoretically (Ditmars(1974), Milgram(1983), Brevik(1996)) and experimentally ((Milgram(1983), Castillejos(1987a), Barbosa(1996)) by many authors in the past three decades. The studies cover a large range of conditions but fail to propose a single model capable of dealing with all possible variations in flow conditions. For the integral approaches, the flow has been divided into three distinct regions where some dominant effects prevail (Milgram(1983)). The buoyancy dominated region is normally referred to as the “Zone of Established Flow”. This will be the region of main interest here.

For flow geometries where two or more plumes are present, the number of works is considerably smaller. A relatively complete work on multiple plume systems is the work of Joo and Guthrie(1992). In this work, the twin bubble plume arrangement flow has been studied both from an experimental and a numerical point of view. Using a tracer technique to quantify the total mixing time – the time interval that 95% of the tracer needs to be mixed in the flow – several plume arrangements were tested. The flow pattern for each arrangement was then numerically reproduced with the help of a κ - ϵ turbulence model. In all numerical calculations, the plumes presented a clear upright position, irrespective of their proximity to the wall. Thus, no sign of the Coanda effect was observed in the numerical computations. Some pictures of the phenomenon, taken by the same author, were however very clear in exhibiting the plume’s deflection. The mathematical modelling of the flow was, therefore, in clear disagreement with the experimental evidence. In this simulation, the action of the bubbles was limited only to the buoyancy term, resulting in a very simple model for the gas phase that could not predict the interaction between the plumes.

As far as the interaction between adjacent bubble plumes is concerned, no analysis

(experimental or theoretical) has been identified by the present authors in literature. The interaction between laminar thermal plumes has been studied using a Mach-Zehnder interferometer (Pera(1975)). For this case, a simple model was developed in order to take into account the deflection angle of the centre lines of the plumes. Pera and Gebhart observed that plane plumes manifest stronger centre line inclinations than axisymmetric plumes.

Arrangements consisting of a single plume developing near to a wall were studied by Menut et al.(1998). This geometry classically defines the Coanda effect; in fact, when Weber and Froude numbers based on the distance between the gas source and the wall were high, the plume exhibited a type of a Coanda effect, bending towards the wall. The angle of deflection was observed to be about 2 degrees.

THE COANDA EFFECT

The definition of the Coanda effect has been clearly stated by Reba(1966) as

“The Coanda Effect is the tendency of a fluid, either gaseous or liquid, to cling to a vertical surface that is near to an orifice from which the fluid emerges”.

An experimental fact is that when two point sources of buoyancy (or momentum) are placed side by side, the two resulting turbulent plumes (or jets) tend to bent towards each other.

For laminar flow, the deflection of the plumes normally results from pressure differences (Pera(1975)). For turbulent flows, on the other hand, the entrained fluid must have a commanding effect on the flow properties. In axisymmetric geometries, the role played by pressure differences must be negligible since the net forces cancel out due to the symmetry.

In the present work, we will shown how a simple model that considers the entrainment coefficient to vary along the periphery of the plume is capable to provide a good prediction of the plume deflection.

EXPERIMENTS

Electro-resistivity sensors built from small needles were simultaneously developed by Neal and Bankoff(1963) and by Nassos(1963). In these studies, almost all efforts were dedicated to the development of the experimental technique rather than to the investigation on the nature of some particular type of flow. Neal and Bankoff used a Nitrogen-Mercury system, whereas Nassos carried out measurements in an air-water system. Serizawa et al.(1975) and Herringe and Davis(1976) gave important contributions to the understanding of the structure of turbulence in internal two-phase bubbly flows. Chesters et al.(1980) were the first to employ the resistivity technique in gas-liquid non-confined flows with a certain degree of success. The authors used electro-resistivity sensors together with laser-Doppler anemometry to describe the characteristics of the liquid and of the gas phases in a bubble plume. Tacke et al.(1985), studying gas stirred steel making processes, used the electro-resistivity sensor technique to make some measurements of the gas phase properties in air-water, Helium-water and Nitrogen-Mercury systems. Castillejos and Brimacombe(1987a,1987b), also aiming at the application of the bubble plume phenomenon in the steel making industry, developed a comprehensive instrumentation based on the resistivity technique to investigate the problem. In 1988, Teyssedou et al. presented a

new AC probe system, together with an analysis of the effect of the geometry of the sensor tip and of other parameters on the performance of the system. More recently, Kocamustafaogullari and Wang(1991), Leung et al.(1992) and Liu and Bankoff(1993) used resistivity sensors to determine local time-averaged gas fraction, interfacial area concentration, bubble rise velocity and bubble pierced length in internal bubbly flows. A recent review on gas stirred steel making processes has been published (Mazumdar(1995)). A numerical analysis of a confined plume compared to experimental results has been presented (Smith(1998)). Finally, Sun et al.(1998) have measured the characteristics of an air plume. The two last ones devised measures by electro-resistivity sensor and laser-Doppler anemometry.

The working principle of the experimental technique is based on the difference between the electrical conductivity(resistivity) of the phases. Since the electrical conductivity of water is much higher than that of air, it is assumed, for practical purposes, that only the continuous phase(liquid) is capable of conducting electrical current. Accordingly to Herringe(1976), resistivity sensors are the most suitable technique for measurements in two-phase mixtures where the continuous phase is conductive. The main adversity of the technique is the existence of an in-stream sensor, which affects the structure of the flow.

In a double channel system (whether AC or DC supply), the difference in electrical resistivity between the phases can be sensed by the electrodes in the two-phase flow so that parameters like the local time-averaged gas fraction, the rise velocity and the pierced length of bubbles can be obtained through the analysis of the output signal.

The measuring system used in this work comprises a signal conditioning module and a double channel needle probe. The signal conditioning module is composed of two identical electronic circuits (one for each channel) connected to the same electrical reference (that can be either the probe sheath or a third electrode immersed in the single phase region). The circuits are fed by a $12VAC$ signal and their main component is the monolithic bipolar integrated circuit $LM1830N$, which was devised for use in fluid measurement and detection systems. An AC supply system was chosen because, according with Teyssedou(1988), it is superior to the DC method. DC systems are subject to problems such as polarisation and electrochemical attack.

The principle of operation can be stated very simply. When the resistance of flow, R_f , increases above a pre-set value, the oscillator signal is coupled to the base of the open-collector output transistor.

The frequency of the oscillator is inversely proportional to the external capacitor value, C_1 . A $220pF$ capacitor was chosen so that an oscillation frequency of $25KHz$ could be provided. The output amplitude from the oscillator is approximately $4V_{BE}$. Thus, when R_f equals the reference resistance, R_{ref} , the detector (which is an emitter base junction) is turned on by a $2V_{BE}$ voltage. The probe is also excited with $2V_{BE}$. The reference resistance, R_{ref} , is coupled to R_f by a blocking capacitor ($C_2 = 0.047 \mu F$) to avoid net DC on the probe.

The collector of the detecting transistor is brought out to pin 9 enabling a filter capacitor ($C_3 = 0.047 \mu F$) to be connected so that the output will be a digital on/off signal depending on the value of R_f . The on/off signal is then brought to a shifter where the voltage is transferred to the level of the digital card input.

The measuring probe was designed as follows. A $0.2mm$ diameter stainless steel wire (upstream electrode) is electrically insulated, with exception of its tip, and embedded in a $0.4mm$ OD $0.2mm$ ID hypodermic tubing (downstream electrode), whose tip is also free of insulation. The length of the electrodes free of insulation is approximately 0.1 mm and

Table 1: Experimental test conditions, two plumes geometry.

Case	s[cm]	q[l/min]	F_r	W_e
i	3.25	1.2	1.12 e-3	0.2910
j	3.25	2.4	4.50 e-3	1.1638
k	6.4	1.2	3.80 e-5	0.0381
l	6.4	2.4	1.52 e-4	0.1524
m	9.05	1.2	6.72 e-6	0.0135
n	9.05	2.4	2.69 e-5	0.0539

the probe tips were shaped to minimise their interference in the flow field. The distance between the electrodes, es is equal to $1.5 \pm 0.15mm$. The co-axial probe type consists of an improvement on the parallel probe type used by Barbosa(1996) in previous works . Due to its symmetric geometry, the co-axial probe interference on the flow is weaker than that of a parallel probe of nearly equal dimensions.

The meaning of parameter R_f (resistance of the flow) is discussed next. The actual value of R_f results from a combination of two factors, the resistance of the probe (that depends on the material from which the probe was made, on the effective electrical contact area and on the distance between the needles and the reference electrode) and the resistivity of the fluid that surrounds it. Each channel has its own R_f , which will be named from this point on as R_{f1} and R_{f2} . The channels are calibrated separately and, due to the reasons explained above, their resistances (R_{f1} and R_{f2}) often assume different values. A detailed calibration procedure is described in Barbosa(1996).

The experimental apparatus is shown in Figure 1. It comprises a water tank, an air injection system, a 2D traversing mechanism and a data acquisition and analysis system. The glass water tank has dimensions 1x1x1 meter and is filled with a 3 gram per litre sodium chloride solution (brine). The air injection system is composed of a mass flow meter and two different injection nozzles (a single 3.2 mm diameter hole and a porous nozzle consisting of thirteen 1.0 mm diameter holes). The data acquisition and analysis system consists of a microcomputer with an interface data acquisition board, an oscilloscope, a signal conditioner module and the electro-resistivity probe. A sketch of the experimental set up can be seen in Barbosa et al.(1996) or in Menut et al.(1998).

The probe is placed perpendicularly to the tank bottom. The water depth is kept constant and equal to 0.85 m. Approximately 15 minutes of continuous gas flow are necessary to guarantee a steady-state condition. Measurements of bubble plume properties are made for several gas flow rate and injection nozzle conditions with the aid of the traversing mechanism. Table 1 summarises the experimental conditions examined.

The data were acquired at a sampling rate of approximately 2.5 kHz and 50 sampling blocks of 10,000 readings Barbosa(1996) for each measured point were sufficient to describe the flow. A very elementary probe calibration was carried out in a vertical pipe and an uncertainty of 10% in the gas fraction results was calculated.

EXPERIMENTAL RESULTS

The general flow pattern for two bent plumes is shown in Figure 1.

The void fraction profiles at different z -stations are shown in Figure 2. The points of maximum void fraction are shown in the Figure as well. They will be taken as our

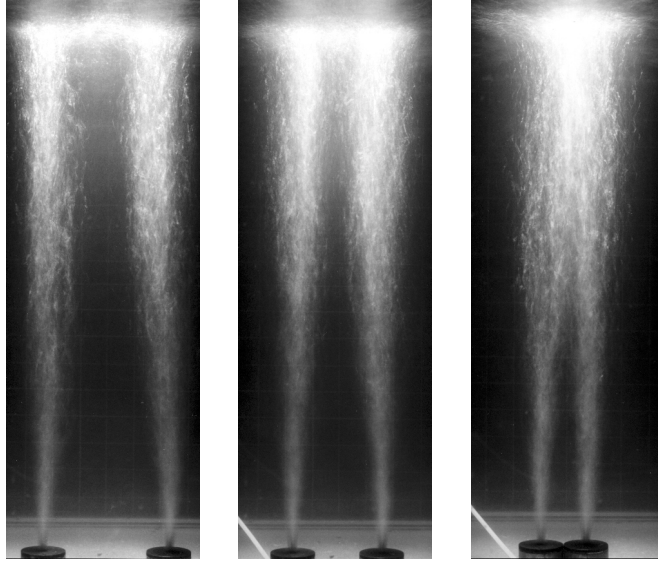


Figure 1: General flow pattern.

reference for the evaluation of the position of the centre line of the plume. From previous studies, we know these points to correspond to the points where the liquid phase velocity is maximum as well. The profile corresponding to the lowest station presents well defined Gaussian curves showing that the plume interaction cannot still be felt at this height. All subsequent profiles, however, present a noticeable deformation due the proximity of the other plume. The points of maximum void fraction are seen to migrate to the centre of the geometrical arrangement, giving origin well downstream to a single plume with a well defined Gaussian shape. The points of maximum void fraction correspond as well to the points of maximum velocity, being, therefore, used to define the centre of the plumes.

The deflection angle of the plumes is shown next in Figure 3 for two different gas injection rates and three different separation distances between the nozzles. This Figure shows that most of the trajectories can reasonably be approximated by a straight line. For the plumes whose distance between each other is large this trend is particularly well defined. We may thus construct graphs for the variation of the deflection angle defined by these straight lines as a function of the Froude number and of the Weber number. These graphs are shown in Figure 4; they show that ϕ increases logarithmically and monotonically with both F_r and W_e according to the two displayed curves. These curves could, perhaps, be approximated by straight lines.

The non-dimensional groups were defined accordingly to

$$F_r = \frac{q^2}{g s^5}, \quad W_e = \frac{\Delta\rho q^2}{\sigma s^3}, \quad (1)$$

where g is the acceleration of gravity, q is the gas flow rate issuing from each source, σ is the surface tension and $\Delta\rho$ is the density difference between the phases. The quantities above are, respectively, the modified Froude, F_r , and Weber, W_e , numbers based on the halved distance between the sources, s or the distance from a wall.

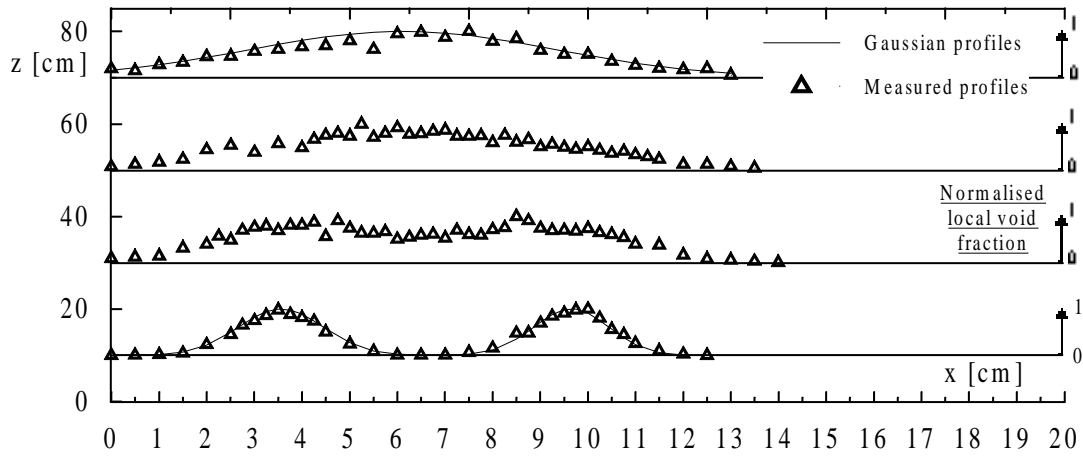


Figure 2. Local void fraction profiles for several stations, $s=3.25$ cm, $q=2.4$ l/min.

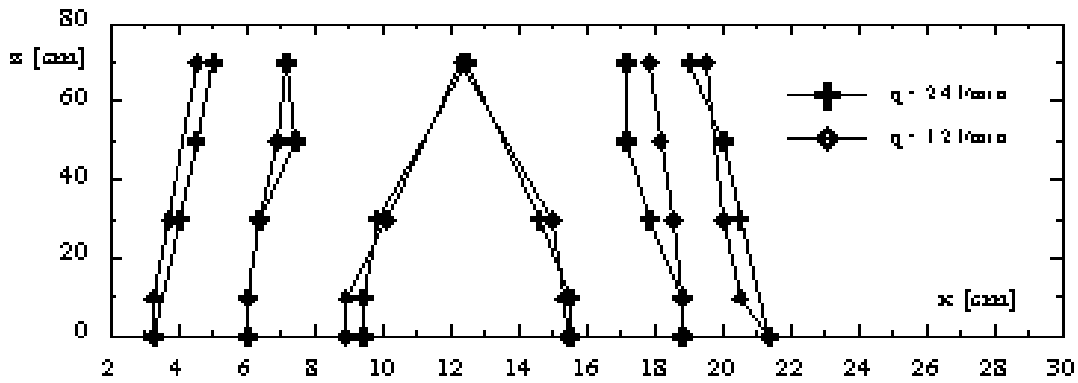


Figure 3. Plume deflection for several gas flow rates and distances from the wall.

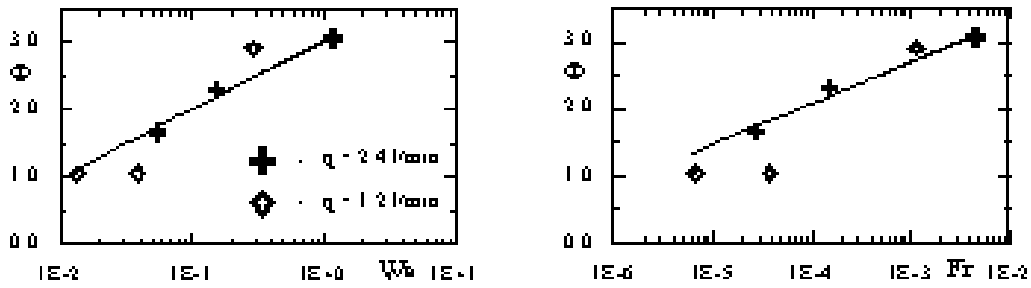


Figure 4. Deflection angle versus Weber and Froude number.

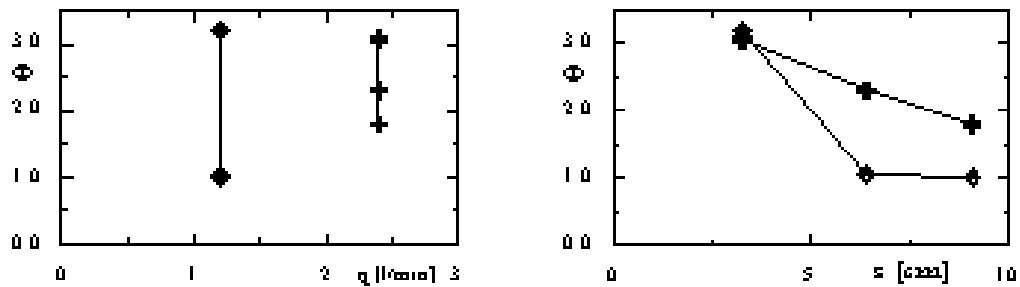


Figure 5. Deflection angle versus flow rate and half distance between the sources.

Although apparently obvious, the above conclusion could not have been arrived at if graphs in dimensional form were used. Figure 5 describes the phenomenon in terms of q and of s . Note that no conclusion can be taken from this Figure regarding the deflection of the plume; the results for q in special do not made any sense.

INTEGRAL THEORY

Mean-flow theories for bubble plumes are integral theories for which the forms of the radial distributions of the velocity and of the density deficiency between the plume and the surrounding fluid are considered to be known in advance. In fact, since the pioneering work of Kobus(1968) to the more recent theories, very little in terms of the formulation has changed. The recent theories have incorporated many novelties, but the basic formulation of the problem remains the same; the governing equations are constructed from the conditions of conservation of gas, conservation of liquid, and the change of momentum flux with buoyancy.

In the present work, the theory of Ditmars and Cederwall(1974) will be used as a basis for our developments. By allowing the entrainment coefficient to vary along the plume periphery, the effect of deflection provoked by an adjacent twin plume can be conveniently modelled. This a very simple premise, which yields very good results.

Since the basic details of the theory can be found in Ditmars and Cederwall(1974), only a brief mention of them will be made here.

The velocity and mean density defect are given by

$$u(x, r) = u_m(x) e^{-r^2/b^2}, \quad (2)$$

$$\rho_a - \rho_m(x) = \Delta\rho_m(x) e^{-r^2/(\lambda b)^2}, \quad (3)$$

where $b(x)$ is the lateral dimension of the plume, ρ_a is the water density and λ is the lateral spread of density deficiency to momentum.

The liquid volume at any elevation and the momentum flux are given respectively by

$$Q = \int_0^\infty 2\pi u r dr = \pi u_m b^2, \text{ and} \quad (4)$$

$$M = \int_0^\infty 2\pi \rho_a u^2 r dr = \frac{\pi}{2} \rho_a u_m^2 b^2. \quad (5)$$

The entrainment assumption is now taken as the explicit starting point of our theory, i.e., it is considered that the inflow velocity at the periphery of the plume is a fraction $\alpha(\theta)$ of the maximum plume centreline velocity according to

$$\frac{dQ}{dx} = \int_0^{2\pi} \alpha(\theta) u_m b d\theta = \alpha_{int} (u_m b). \quad (6)$$

Then, using Boussinesq approximation, the equations of conservation of mass, x-momentum and buoyancy can be written as

Table 2: Plume deflection angle.

Case	i	j	k	l	m	n
ϕ_{exp}	2.9	3.0	1.1	2.3	1.1	1.7
ϕ_{theor}	2.5	3.2	2.3	2.4	2.3	2.3

$$\frac{d(\pi u_m b^2)}{dx} = \alpha_{int} (u_m b). \quad (7)$$

$$\frac{d(\pi u_m^2 b^2)}{dx} = \frac{2gq_0 H_0}{(H_0 + H - x)(u_m(1 + \lambda^2)^{-1} + u_b)}, \quad (8)$$

$$\pi \Delta \rho_m \lambda^2 b^2 \left(\frac{u_m}{1 + \lambda^2} + u_b \right) = \frac{\rho_a q_0 H_0}{(H_0 + H - x)}. \quad (9)$$

Now, we consider that the bending of the plume is primarily due to an inhibition of the entrainment coefficient in the part of the plume which is nearer to the other. We also consider that all transversal momentum entrained in the plume is retained by its elements as they rise. If M_c denotes the transversal entrained momentum, then

$$M_c = \int_0^x \int_0^{2\pi} \rho_a (\alpha(\theta) u_m b) \alpha(\theta) u_m \cos(\theta) d\theta dx, \quad (10)$$

and the plume deflection angle can be approximated by $\tan(\phi) = M_c/M$.

In the present work, $\alpha(\theta)$ has been approximated by

$$\alpha(\theta) = \frac{\alpha_{max} - \alpha_{min}}{\pi} \theta + \alpha_{min}, \quad 0 < \theta < \pi \quad (11)$$

$$\alpha_{min} = 0.06 - 1.15 W_e, \quad \alpha_{max} = 0.065. \quad (12)$$

We have, thus, proposed a very simple linear correlation for the prediction of the entrainment coefficient behaviour.

The results are shown in Table 2.

It is clear from Table 2 that the results are good provided W_e number is not too small. In fact, cases k and m were the only ones where the model did not show to be appropriated. Under those conditions, W_e is really too small and difficult to incorporate in the theory.

CONCLUDING REMARKS

The present work has established a firm connection between the bending angle of a bubble plume and the values of F_r and W_e numbers. The work has been important in identifying some relevant parameters to the problem and in working out a strategy to determine values of the entrainment coefficient in future more sophisticated formulations of the problem. Also, a very simple theory based on integral methods has been advanced which provides good results.

Acknowledgements. The first author thanks the Brazilian National Research Council (CNPq) for the award of a research fellowship according to Project No 831024/98-4. The work was financially supported by the CNPq through grant No 350183/93-7.

REFERENCES

- Barbosa, J. R. J. and Bradbury, L. J. S., 1996, In Proc. 6th ENCIT/LATCYM, Florianopolis, 1073.
- Brevik, I. and Killie, R., 1996, Int. J. Multiphase Flow, No. 22.
- Castillejos, A. H. and Brimacombe, J. K., 1987a, Metall. Trans. B, No. 18B.
- Castillejos, A. H. and Brimacombe, J. K., 1987b, Metall. Trans. B, No. 18B.
- Ditmars, J. D. and Cederwall, K., 1974, In Proc. Coastal Engng. Conf., Copenhagen.
- Herringe, R. A. and Davis, M. R., 1976, J. Fluid Mech., No. 73.
- Joo, S. and Guthrie, R. I. L., 1992, Metall. Trans. B, No. 23B.
- Kobus, H. E., 1968, Proc. Coastal Engng. Conf., London.
- Kocamustafaogullari, G. and Wang, Z., 1991, Int. J. Multiphase Flow, No. 17.
- Leung, W. H., Revankar, S. T., Ishii, Y., and Ishii, M., 1992, Int. J. Heat Mass Transfer, No. 38(3).
- Liu, T. J. and Bankoff, S. G., 1993, Int. J. Heat Mass Transfer, No. 36(4).
- Mazumdar, D. and Guthrie, I. L., 1995, ISIJ International, No. 35(1).
- Menut, P. P. M., Barbosa Jr., J. R. and Silva Freire, A. P., 1998, 6o Brazilian Nat. Meeting on Thermal Sciences (6o ENCIT).
- Milgram, J. H., 1983, J. Fluid Mech., No. 133.
- Nassos, G. P., 1963, Technical Report 9, Argonne Report ANL – 6738.
- Neal, L. G. and Bankoff, S. G., 1963, AIChE J., No. 9.
- Pera, L. and Gebhart, B., 1975, J. Fluid Mech., No. 68.
- Reba, I., 1966, Sci. Am., No. 214.
- Smith, B. L. and Milelli, M., 1998, In Third Int. Conf. on Multiphase Flow, Lyon.
- Sun, K. X., Zhang, M. Y., and Chen, X. J., 1998, In Third Int. Conf. on Multiphase Flow, Lyon.
- Tacke, K. H., Schubert, H. G., Weber, D. J., and Schwerdtfeger, K., 1985, Metall. Trans. B, No. 16B.
- Teyssedou, A., Tapucu, A., and Lortie, M., 1988, Rev. Sci. Instrum., No. 59(3).